Desalination and Water Treatment
www.deswater.com

doi: 10.5004/dwt.2023.29534

293 (2023) 170–181
May

Photodegradation and mineralization of ciprofloxacin by consecutive application UV/iodide process and biological treatment

Norouz Mahmoudi[a,b,c], Ahmad Jonidi Jafari[a,b], Mahdi Farzadkia[a,b], Majid Kermani[a,b], Amir Sheikhmohammadi[d], Hasan Pasalari[a,b], Ali Esrafili[a,b,*]

[a]*Research Center for Environmental Health Technology, Iran University of Medical Sciences, Tehran, Iran, emails: a_esrafily@yahoo.com (A. Esrafili), m.n.noroz@gmail.com (N. Mahmoudi), jonidi.a@iums.ac.ir (A.J. Jafari), farzadkia.m@iums.ac.ir (M. Farzadkia), majidkermani@yahoo.com (M. Kermani), hasanpasalari1370@gmail.com (H. Pasalari)*
[b]*Department of Environmental Health Engineering, School of Public Health, Iran University of Medical Sciences, Tehran, Iran*
[c]*Health Research Center, Life style Institute, Baqiyatallah University of Medical Sciences, Tehran, Iran*
[d]*Department of Environmental Health Engineering, School of Health, Khoy University of Medical Sciences, Khoy, Iran, email: a_sheikhmohammadi@khoyums.ac.ir*

Received 6 December 2022; Accepted 31 March 2023

ABSTRACT

This research was developed to examine the progressive degradation process of ciprofloxacin (CIP) via reductive species generated in iodide excitation under ultraviolet light as advanced reduction processes. The highest CIP degradation (98.46%) were achieved under optimal condition: pH = 9, CIP:iodide molar ratio = 2:1, and reaction time = 30 min. In UV/iodide process, the reaction rate constant (k_{obs}), reaction rate (r_{obs}), range were 0.182–0.0351 min^{-1}, and 9.135–7.02 $mg{\cdot}L^{-1}$, respectively. Moreover, energy consumption (E_{EO}) was calculated using two methods of kinetics and International Union of Pure and Applied Chemistry (IUPAC). The results indicated that when CIP concentration increases from 50 to 200 $mg{\cdot}L^{-1}$, the amount of E_{EO} increases from 1.54 to 8.02 $kWh{\cdot}m^{-3}$ at kinetic model. In addition, in the IUPAC model. The energy consumption increased from 1.22 to 6.48 $kWh{\cdot}m^{-3}$. Gas chromatography–mass spectrometry was used to study the intermediate products and probable photodegradation routes of CIP in the UV/iodide process; most of the intermediates were calcified into simple linear molecules such as acetic acid ($C_2H_4O_2$), formate (CHO_2^-), and formaldehyde (CH_3OH), and then to CO_2, H_2O, NH_4^+, and NH_3. The modified Kirby–Bauer disc diffusion test was used to investigate bacterial inhibition, the starting concentration of CIP without treatment was lowered from 39 to 11.4 mm after 30 min of reaction time. This decrease in bacterial growth inhibition and intermediate production suggests that the UV/iodide method produces effluent with a high biodegradability. After 30 min, the UV/iodide process led to decreased chemical oxygen demand (COD) by 37.5%. Within 11 h, the COD removal efficiency reached 63.8% (130 to 47 $mg{\cdot}L^{-1}$) when the biological reactor as post-treatment was run at an mixed liquor suspended solids (MLSS) concentration of 1,000 $mg{\cdot}L^{-1}$. However, in case of MLSS concentration (3,000 $mg{\cdot}L^{-1}$), the COD removal efficiency increased to 78.4% (from 185 to 39.7 $mg{\cdot}L^{-1}$), while, 88.16% COD removal efficiency was obtained at an MLSS dosage of 5,000 $mg{\cdot}L^{-1}$ (from 245 to 29 $mg{\cdot}L^{-1}$).

Keywords: Iodide; Photoreductive; International Union of Pure and Applied Chemistry; Bacterial susceptibility test; Biological treatment

* Corresponding author.

1. Introduction

The antibiotic contamination is considered as a serious threat to human and ecological environment; it has attracted widespread attention all over the world [1,2]. About 100,000–200,000 tons of antibiotics are using in the world every year. Given the volume of their consumption, digestion and metabolism in the body, the remaining are excreted in the form of their main compounds or their metabolites (5%–90%) from the human or animal body into the environment and consequently enter directly and indirectly into surface and underground water sources [3–5]. If not properly treated, wastewater can harm humans, aquatic animals and all organisms, especially when contaminants enter the food chain and directly or indirectly enter the bodies of living organisms [6]. Among wastewater pollutants, antibiotics are one of the most important causes of water pollution and are not routinely monitored because they are in the category of emerging pollutants (EPs) [7,8]. Thus, many antibiotics are resistant to microorganisms in terms of high solubility and refractory nature, which cause inefficient removal in biological treatment and lead to the continuous discharge of these contaminants into the environment [9]. Ciprofloxacin (CIP) is an antibacterial agent with an extended usage in the human, the animal husbandry and aquaculture [10–12]. Unfortunately, as it is difficult to degrade in the natural environment, CIP is increasingly being detected in water bodies [13]. Some studies have shown that ciprofloxacin (CIP) has been detected in water environments such as urban wastewater 6.45 [14], hospital wastewater 228 [15], and in the pharmaceutical industry effluent with concentration of 7,900 $\mu g \cdot L^{-1}$ [16]. Therefore, there is an urgent need to discover an effective and appropriate strategy to remove the antibiotics from natural water. Ultrasonic [17], electrolysis [18], photocatalytic [19], adsorption [20], catalytic ozonation [21,22], UV/H_2O_2 [23], UV/iodide/ZnO [24], MgO-PAC [25], persulfate activated magnetic Fe_3O_4/graphene oxide [26] and other methods have been widely used to degradation of persistent organic pollutants)POPs) and emerging contaminants (ECs) in aqueous medium. Nowadays, the advanced reduction processes has become a hot topic in the field of water treatment and grasp much attention by many researchers due to its high reactivity, free radical generation, non-toxicity and non-sludge production, and use them in semi-industrial and industrial scale [27]. The development of highly efficient technologies, such as various advanced reduction processes (ARPs) produced by the stimulation of anions such as sulfite [28], iodide [29], carboxyl [30], to the generation of reducing species have been studied for the antibiotic's degradation. Many studies have focused the emission of electron hydrated (e^-_{aq}) from iodide into the solvent and have concluded that via the process of "charge transfer to solvent modes (CTTS)", it can effectively produce e^-_{aq} on a femto-second time scale [31,32]. As a powerful nucleophilic, it has the potential to reduce the standard voltage to –2.9 and has so far reduced the degradation of various pollutants such as dexamethasone phosphate [29], chrome precipitation [30], nitro-aromatic compounds (NACs) [33], etc [34–37] was applied. The advantage of advanced reduction processes over advanced oxidation processes in this research: The presence of halogen in the structure of cyclic materials is considered as a barrier for decomposition by oxidation processes; breaking the carbon–halogen bond requires very high energy, while reduction processes are easily able to break this bond [38]. Due to their high electronegativity, halogens act as a very strong protector for the benzene (aromatic) ring, and oxidation processes cannot be suitable for this case due to their high resistance to this electronegativity. They have no resistance against the electronegativity of halogen atoms and can easily be separated by giving electrons to these atoms and attack the carbon ring [39]. The purpose of the combination of two biological processes and advanced reduction is the complete decomposition and mineralization of the pollutant. Due to the fact that iodide ion has a good performance for the advanced reduction process and on the other hand, it does not cause disturbance in biological processes, it makes it possible to use two processes consecutively. The use of the advanced reduction pretreatment process for the biological process can help improve biological degradability and appropriate mineralization as a completely environmentally friendly process. Consequently, the fundamental purpose for this paper were to (1) assessment the elimination of CIP by the reductive species generated with iodide excitation under UV irradiation; (2) determination the effects of various operational parameters; (3) examine the reaction kinetic; (4) determination the intermediate by-products; (5) bacterial susceptibility test; (6) determination of improvement the biodegradability; (7) and assessment of biological post treatment.

2. Materials and methods

2.1. Photoreductive reactor setup

A batch photoreactor with UV lamps in different irradiation flux 2, 3 and 4 $mW \cdot cm^{-2}$ (powers 11, 8 and 6 W) in the range λ_{max} = 254 nm placed in a quartz sleeve (as a covering that does not absorb ultraviolet light) was used in the present study. The quartz sleeve was placed in center of steel chamber and CIP solutions were entered in space between them, which is the reaction zone. Eventually all of these components were placed in a larger chamber, cooled by water (cooling tank). All the pilot are shaken by an orbital motion. Fig. 1a shows a schematic of the pilot used. When the effluent of advanced UV/iodide reduction process has the necessary indicators (BOD_5/COD ≥0.4, bacterial susceptibility test and intermediate products), it enters the aerobic biological system for further biological treatment and mineralization (Fig. 1b) [40]. The aerobic bioreactor was ultimately used to chemical oxygen demand (COD) removal. Three distinct reactors with variable concentrations of mixed liquor suspended solids (MLSS) (1,000; 3,000 and 5,000 $mg \cdot L^{-1}$) and aerated with the appropriate nutrients were run. The effluent was filtered using a 0.45 μm filter for further analysis.

2.2. Analytical methods, identification of intermediate compounds and photodegradation pathways

The CIP concentration was measured in the tests using a high-performance liquid chromatography (HPLC; using a

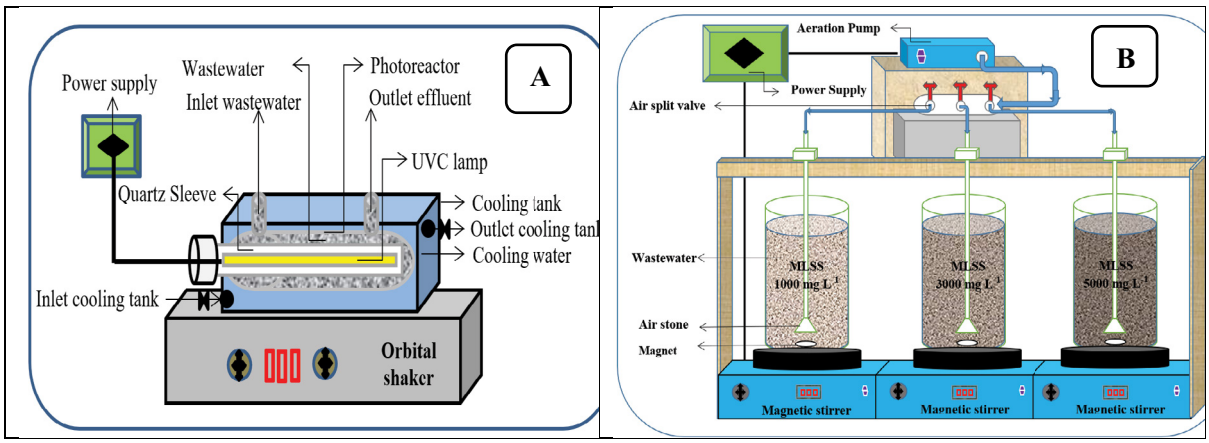

Fig. 1. Schematic of (a) photoreductive and (b) biological reactor.

Shimadzu 2010HTC Instrument, England) outfitted with a PerkinElmer C18 column, England (flow rate was 1 mL·min^{-1}) and a spectrophotometer with a 280 nm wavelength. Distilled water with HPLC grade (60%) and acetonitrile (40%) was used as the mobile phase. The mineralization and degradation efficiency CIP were calculated by Eqs. (1) and (2):

$$\text{CIP degradation} = \frac{\text{CIP}_0 - \text{CIP}_t}{\text{CIP}_0} \quad (1)$$

$$\text{CIP mineralization} = \frac{\text{COD}_0 - \text{COD}_t}{\text{COD}_0} \quad (2)$$

where in COD test used to evaluation of mineralization [41]. Also, gas chromatography–mass spectrometry (GC-MS) used to study CIP intermediates and pathways.

2.3. Kinetic model, energy and effective cost analyses

To study CIP photodegradation in solutions, pseudo-first-order kinetic model was applied according to Eqs. (3) and (4):

$$\ln\frac{C_t}{C_0} = -K_{\text{obs}}t \quad (3)$$

$$r_{\text{obs}} = -k_{\text{obs}}C_{\text{CIP}} \quad (4)$$

where k is the constant coefficient of reaction rate.

Electrical energy per order (E_{EO}) figures have been proposed according the International Union of Pure and Applied Chemistry (IUPAC) in order to facilitate better comparison of UV lamp-based processes. 90% of the contaminants in 1 m^3 of wastewater are destroyed by E_{EO} [29].

$$\text{IUPACE}_{\text{EO}} = \frac{P \times t \times 1{,}000}{V \times 60 \times \log\frac{C_i}{C_f}} \quad (5)$$

By combining Eqs. (3) and (5), E_{EO} obtains based on kinetic equation [42].

$$\text{Kinetic } E_{\text{EO}} = \frac{P \times 38.4}{V \times K_{\text{obs}}} \quad (6)$$

2.4. Investigation the anions and role of reducing and oxidizing species

In this stage, we surveyed the interaction between inorganic water anions, such as chloride, nitrate, bicarbonate, and sulfate, on ARP reactive species. Additionally, the function of tert-butyl alcohol as a scavenger oxidizing species and carbon disulfide and carbon tetrachloride scavengers were employed to determine the involvement of reducing species [43].

2.5. Antibiotic susceptibility assay

The modified Kirby–Bauer method according to the Clinical & Laboratory Standards Institute (CLSI) guidelines was used to determine the bacterial susceptibility to antibiotic. Based on previous studies, *Escherichia coli* was shown to be sensitive to fluoroquinolone antibiotics, which is an indicator for evaluating the bacterial susceptibility of CIP and its intermediate products can be used during the light degradation process (He et al. [44] and Singh et al. [45]).

2.6. Indicators for improving biodegradability and mineralization

The COD index was utilized to calculate the mineralization level. Samples containing CIP were measured for COD and biochemical oxygen demand (BOD) using the methods 5220B and 5210B described in the standard procedure [46].

2.7. Biological post-treatment

The settings under which the rate of degradation was greatest were chosen as the advanced UV/iodide reduction process' ideal conditions at this point after testing the effectiveness of the process in the reduction of CIP antibiotics. To introduce the effluent from the advanced UV/iodide reduction process into the biological system, the BOD/

COD ratio was computed. In order to further mineralize, the advanced UV/iodide reduction process' effluent entered the aerobic biological system under ideal circumstances and with a BOD_5/COD ratio of 0.4 [47]. On a lab scale, experiments were conducted sporadically (batch) in three reactors with various MLSS concentrations (1,000; 3,000 and 5,000 mg·L^{-1}). After filtering the sample via 0.45 μm filter, the remaining COD was determined.

3. Results

3.1. Effect of pH on removal of CIP by UV/iodide process

Fig. 2 illustrates the impact of pH on the effectiveness of CIP removal using the UV/iodide method in the pH range of 3 to 11. Initial CIP concentration was 50 mg·L^{-1}, and the CIP:iodide molar ratio was 2:1. Diagrams used in the research of pH conditions may be seen to reveal how this pollutant decomposes at different rates that are noticeably different. According to Fig. 2, the removal effectiveness of CIP increased as the pH rose, the highest removal efficiency (98.46%) was observed at pH 9, compared to 54.26% for UV alone (without the addition of iodide). After 30 min of reaction time, CIP removal efficiency reduced by 83.34%, and at pH 11, the removal efficiency decreased in comparison to pH 9. However, the greatest CIP removal effectiveness at pH 3 after 30 min of reaction time was 18.8%. In addition, at pH values of 8.5, it can cause increasing of the disproportionation of I_2 iodine to iodide ions I^- and IO_3^- according to Eq. (15), more I^- recycling and less production of I_2 and triiodide (I_3^-) [Eqs. (11) and (12)], which produces more e^-_{aq} [Eqs. (1)–(3)] and reduces its consumption [Eqs. (7)–(11)] [48].

$$I^{\bullet} + I^{\bullet} \rightarrow I_2 \quad (7)$$

$$I^- + I_2 \rightarrow I_3^- \quad (8)$$

$$e^-_{aq} + I_2 \rightarrow 2I_2^- \quad (9)$$

$$e^-_{aq} + I_3^- \rightarrow I_2^- + I^- \quad (10)$$

$$3I_2 + 6OH^- \rightarrow 5I^- + +IO_3^- + 3H_2 \quad (11)$$

Botlagodra et al. [49] studied an advanced reduction process to remove bromine. They showed that alkaline pH showed better results for the advanced reduction process compared to acidic pH. The authors did not observe any significant differences between pH 9 and 11. In 2021, Milh et al. [50] investigated the degradation of CIP using sulfite-based reduction; the authors reported that at pH 7–9, CIP present in neutral (CIP^0) and generation of hydrated electrons (e^-_{aq}) in these conditions and failure to convert it to other species with less reactivity. Also, they found that increasing the pH from 3 to 8.5 improved degradation rate. However, with further increase in pH, CIP degradation decreased. They concluded that deprotonation of amino groups in the CIP piperazine ring enhances the electron donor property of the CIP molecule and reduces the CIP barrier.

3.2. Impact of molar ratio on the UV/iodide process for CIP photodegradation

The findings on the effects of various CIP:iodide molar ratios in the UV/iodide process (taking into account CIP concentration of 50 mg·L^{-1}, pH 9, and reaction period 0–30 min) are shown in Fig. 3. According to Fig. 3, the highest removal efficiency (98.46%) found at a 2:1 molar ratio between CIP and iodide. The increase in efficiency varies based on the kind of contamination and is greatly reliant on whether it is proportionate to the bonds in the CIP molecule or the target molecule. Fig. 3 depicts the pattern of CIP breakdown as the iodide concentration changes. As can be observed, the removal effectiveness is higher in the 2:1 CIP:iodide molar ratio compared to in other molar ratios. This is because the CIP:iodide molar ratio plays an important role in the production of reducing species. However, excessive increase can lead to iodide recombination and various other species (I_2, HOI, I_3^-, IO_3^-) that are much less effective [27]. The key point is that when the iodide content is lower than the CIP, too much iodide reacts with these materials and is therefore not exposed to UV, resulting in significantly reduced e^-_{aq} production [51]. These iodide derivatives can react with intermediate organic matter or CIP and converted back to iodide. If the amount of iodide is lower than that of CIP, a significant amount of it will naturally be reacted with organic matter and the reaction with photons will be reduced, resulting in less reducing species

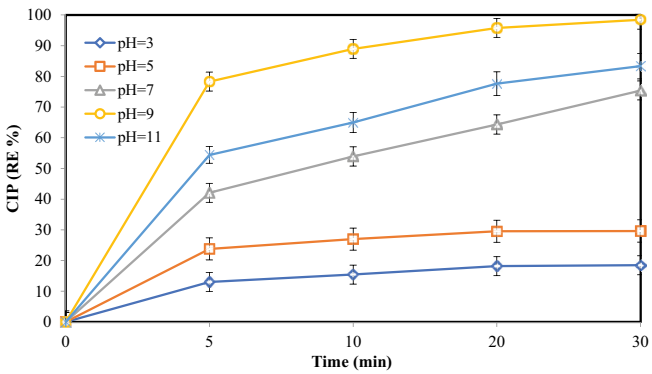

Fig. 2. Impact of pH on the UV/iodide process for ciprofloxacin photodegradation in ideal condition.

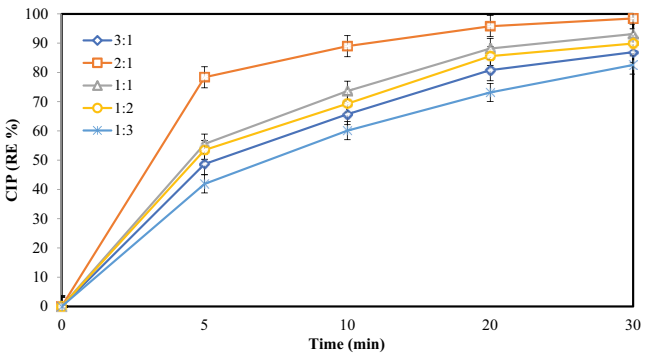

Fig. 3. Impact of molar ratio on the UV/iodide process for ciprofloxacin photodegradation in ideal condition.

such as e^-_{aq} [51]. Based on Beer–Lambert's law, increasing the anion concentration due to increased UV adsorption leads to an increase in reactive species, and thus better decomposition efficiency [52,53]. The result presented in this study is very similar to the study conducted by Jung et al. [54]. Mahvi et al. [29] reported the ideal DexP:KI molar ratio of 2:0.9 at pH 9 as the optimal conditions for elimination of dexamethasone phosphate by UV/iodide method [29]. The ideal PFOA:KI molar ratio at pH 9 was established by Park et al. [13] when they conducted perfluoroalkyl removal using the UV/iodide technique. Yu et al. [55] found that by increasing the sulfite dose from 1 to 5 mM, the constant rate of degradation of 2, 4 dichlorophenol by the UV/sulfite process increased significantly. While further increase of initial sulfite concentration to 16 mM did not lead to further increase of k_{obs}. They explained that the initial increase in sulfite concentration in terms of the greater uptake of UV light by sulfite and the production of more reductive species responsible for degradation led to higher removal efficiencies with a proportional increase in k_{obs}. However, at higher reductive species concentrations, the generated reductive species begin to react with each other and with the intermediates produced during the process (they now act as scavengers), leading to the consumption of more reductive species. Hence, it inhibits a proportional increase in the rate of destruction.

3.3. Impact of UV lamp radiation flux on the UV/iodide process for CIP photodegradation

The findings of the investigation and comparison the effects of UV lamp radiation flux on CIP removal effectiveness in the range of 50 mg·L^{-1} in the time range of 0–30 min and CIP:iodide molar ratio of 2:1 are shown in Fig. 4. By increasing the lamp radiation flux from various irradiation fluxes of 2, 3, and 4 mW·cm^{-2}, respectively, the degradation rate of CIP increased from 52.16%, 72.46%, and 98.46% in 30 min.

3.4. Impact of CIP concentration, kinetics and cost-effectiveness

According to the findings of Fig. S1, the influence of initial CIP concentration on removal effectiveness in four CIP concentrations of 50, 100, 150 and 200 mg·L^{-1} are compared. The results are provided in Table 1 and Fig. 5. When the CIP concentration was increased the degradation rate of CIP fell from 98.46% to 66.7%, respectively. According to Table 1, at all concentrations, the rate of CIP degradation reduced as reaction time increased from 0 to 30 min. With a rise in CIP concentration from 50 to 200 mg·L^{-1}, the reaction rate constant (k_{obs}) and reaction rate (r_{obs}), respectively, were found to be 0.1892–0.0351 min^{-1} and 9.46–7.02 mg·L^{-1}·min^{-1}. Additionally, the amount of energy consumed was calculated using the kinetics and IUPAC methods. The results show that as CIP concentration rises from 50 to 200 mg·L^{-1}, the kinetic model's energy consumption increases from 1.54 to 8.02 and the IUPAC model's increases from 1.22 to 6.48 kWh·m^{-3} of treatment. According to Rasolevandi et al. [29], the amount of energy required for the UV/iodide process to degrade dexamethasone phosphate increased from 1.45 to 8.95 kWh·m^{-3} when the concentration of dexamethasone phosphate increased from 10 to 100 mg·L^{-1}. Also, in the research of Dolatabadi et al. [56] on the electrochemical degradation of pesticides using Ti/SnO_2-Sb_2O_3/PbO_2/Bi electrode the

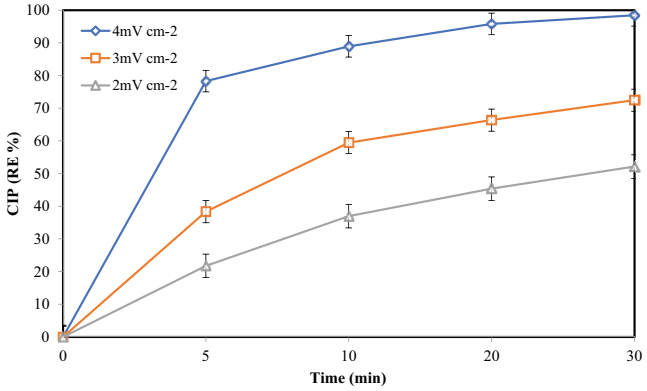

Fig. 4. Impact of UV lamp intensity on the UV/iodide process for ciprofloxacin photodegradation in ideal condition.

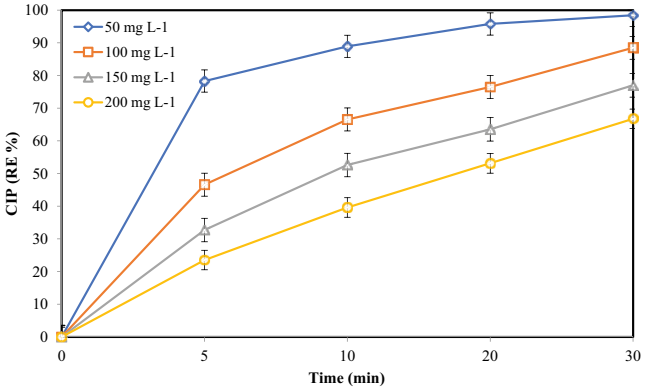

Fig. 5. Impact of concentration on the UV/iodide process for ciprofloxacin photodegradation in ideal condition.

Table 1
Pseudo-first-order kinetic model and E_{EO} data

Ciprofloxacin (mg·L^{-1})	R^2	k_{obs} (min^{-1})	r_{obs} (mg·L^{-1}·min^{-1})	Kinetic E_{EO} (kWh·m^{-3})	Figure-of-merit E_{EO} (kWh·m^{-3})
50	0.9918	0.1892	9.46	1.54	1.22
100	0.9909	0.0777	7.77	3.75	3.05
150	0.9703	0.0486	7.29	5.75	4.77
200	0.9821	0.0351	7.02	8.02	6.48

current density was 6.0 mA·cm^{-2} and at 60 min reaction time the energy consumption was 5.1 kWh·m^{-3} [56].

3.5. Anions Impact on the UV/iodide process for CIP photodegradation

The main anion found in surface and groundwater, which might come into contact with reactive species in AORPs and lessen their reactivity. As shown in Fig. 6, assessment demonstrates that the examined anions in the photodegradation function of CIP in the order of 100% (absence of any anion) in the amount of decreases 58.49% when utilizing the ideal circumstances of UV/iodide, pH 9, and the CIP:iodide molar ratio of 2:1 (in the presence of nitrate). Particularly, after 30 min of reaction time, the addition of nitrate, bicarbonate, chloride, and sulfate decreased the photodegradation of CIP by 41.51%, 30.09%, 21.25%, and 28.32%, respectively. The process' most productive anion in this investigation was nitrate. The acid dissociation constant (ka) of the majority of nitrates may be the primary cause of this [57]. Additionally, as shown in Eq. (12), the presence of N atoms in the CIP molecule is oxidized once the CIP molecule is broken down by the assault of radicals on NO_3 [58]. According to the Le Chatelier principle and the law of balance, NO_3 production might decrease process effectiveness [59,60].

$$C_{16}H_{15}N_5O_7S_2 + HO^{\bullet} \rightarrow NO_3^- + \text{products} \quad (12)$$

e^-_{aq} can react with anions according to Eqs. (13)–(16) [41,61]:

$$HCO_3^- + e^-_{aq} \rightarrow HCO_3^{-2} \quad (13)$$

$$Cl^- + e^-_{aq} + H^+ \rightarrow HCl \quad (14)$$

$$NO^{3-} + e^-_{aq} \rightarrow \left(NO_3\right)^{"2-} \quad (15)$$

$$SO_4^{2-} + e^-_{aq} \rightarrow SO_4^{3-} \quad (16)$$

3.6. Investigation of the reaction mechanism of CIP degradation by UV/iodide process

By sealing the species reducing carbon disulfide and carbon tetrachloride, the effects of reducing agents were investigated. As reducing species scavengers, the addition of carbon tetrachloride and carbon disulfide inhibits photodegradation efficiency by 40% and 47%, respectively, as shown in Fig. 7. As a result, decreasing species are crucial to the photodegradation of CIP. Tert-butyl alcohol (an oxidative species scavenger) was also added to the reaction medium to identify the potential impact of oxidizing species, which decreased the yield by up to 4%. This implies that photocatalytic reduction is the reaction's mechanism.

3.7. Intermediate products and degradation pathways of CIP

In order to look into potential photovoltaic pathways of CIP in the UV/iodide process, intermediate products and degradation pathways of CIP UV/iodide effluent at photodegradation time of 30 min were analyzed using GC-MS. The photodegradation process starts when a hydrogen atom replaces the fluorine ring under the influence of a reducing agent. However, it is obvious that the reducing agent plays a crucial part in the photodegradation of CIP. Additionally, Table 2 lists the existence of photodegradation intermediates. Fig. 8 depicts modifications made to CIP's structure and during its transformation into mediators. Fig. 8 depicts the main pathways of CIP defluorination and hydrogen fluoride acid release as the process of photodegradation starts. In order to break down the ring and produce the intermediates I_1, I_2, and I_3, CIP reacts with reductive species like e^-_{aq}. The remaining materials can then be broken down by other reductive species, producing compounds devoid of the benzene ring. Then, these compounds transform into quickly biodegradable linear and simple organic compounds like acetic acid (I_7:$C_2H_4O_2$), formaldehyde (I_8:CH_2O), and formate (I_9:CHO_2^-), before mineralizing to CO_2, H_2O, NH_4^+, and NH_3 and being eliminated from the reaction medium [51]. Iodide intermediate products have been seen in some studies, but this study did not find any of these products [62]. The low reactivity of iodide radical species toward reductive species may be the cause of this. Iodide ion functions as a catalyst

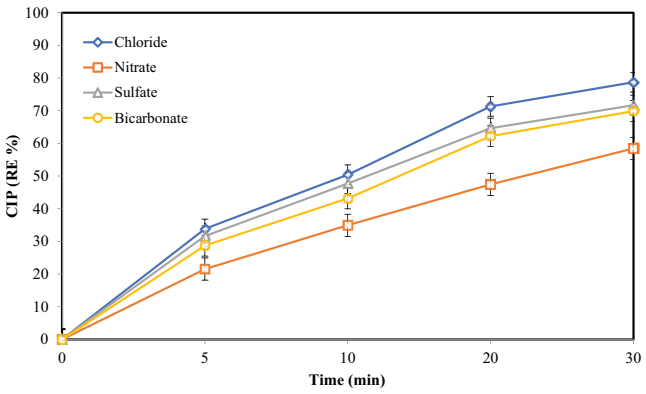

Fig. 6. Impact of anions on the UV/iodide process for ciprofloxacin photodegradation in ideal condition.

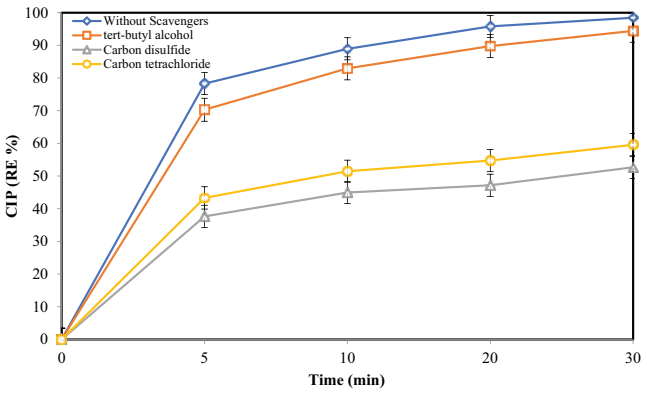

Fig. 7. Impact of different inhibitors on the UV/iodide process for ciprofloxacin photodegradation in ideal condition.

Table 2
Summary of intermediate compounds produced in the UV/iodide process

Intermediates symbol	Molecular weight	Chemical formula	Molecular name	References
I_1	86.14	$C_4H_{10}N_2$	Piperazine	(Liu et al. [63])
I_2	243.26	$C_{14}H_{13}NO_3$	1-Cyclopropyl-6-methyl-4-oxo-1,4-dihydroquinoline-3-carboxylic acid	No
I_3	329.40	$C_{18}H_{23}N_3O_3$	(E)-3-(cyclopropylamino)-2-(3-methyl-4-(piperazin-1-yl) benzoyl)acrylic acid	No
I_4	88.15	$C_4H_{12}N_2$	N^1,N^2-dimethylethane-1,2-diamine	No
I_5	155.15	$C_7H_9NO_3$	(E)-3-(cyclopropylamino)-2-formylacrylic acid	No
I_6	87.17	$C_5H_{13}N$	2-Methylbutan-1-amine	No
I_7	60.05	$C_2H_4O_2$	Acetic acid	(Wang et al. [64])
I_8	30.03	CH_2O	Formaldehyde	(Kamath et al. [65], Sarkhosh et al. [38])
I_9	45.02	CHO_2^-	Formate	No

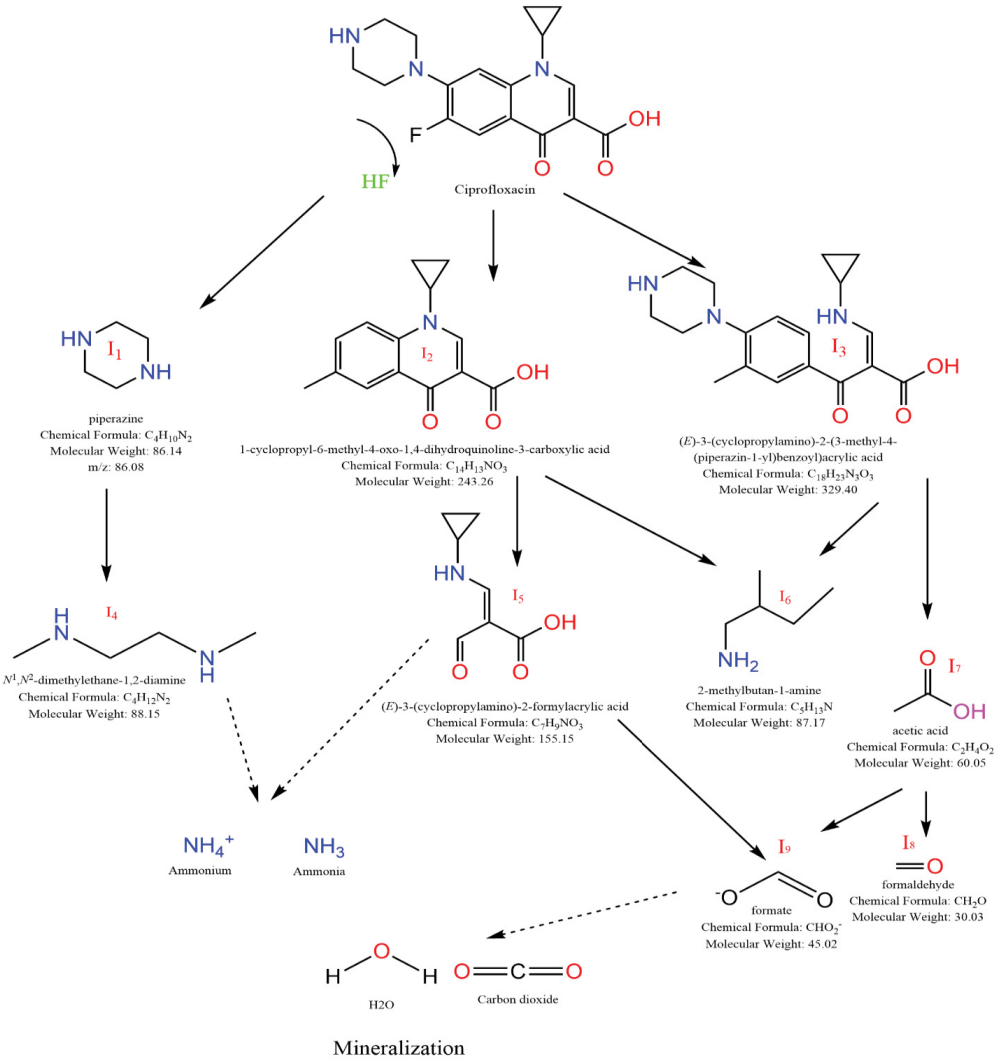

Fig. 8. Possible reaction pathway and intermediate compounds produced in photodegradation of ciprofloxacin in the UV/iodide ARP.

like ferrate(VI), but it is more successful at producing reducing species [66].

3.8. Susceptibility of bacteria and antibiotic activity

Samples were taken at various periods to test the bacterial susceptibility of the CIP UV/iodide process treatment effluent (0–30 min). *Escherichia coli* sensitivity to CIP and intermediate were evaluated using the modified Kirby–Bauer disc diffusion test technique, which was used to study antibiotic-induced bacterial inhibition. According to Fig. 9 from this investigation, bacterial inhibition decreased from 39 mm in the initial concentration of CIP without treatment to 11.4 mm after 30 min of reaction time, demonstrating that the treated effluent was not harmful to bacteria. The initial inhibitory zone for 10 mg·L^{-1} CIP in a research looking at the removal of CIP by Bi_2WO_3 nanoparticles under visible light conditions was 19, and after 30 min the reaction time reached 8 [67]. Additionally, the drug activity of an unrefined solution containing 50 mg·L^{-1} of chloramphenicol was assessed at various times during the study of chloramphenicol removal by UV/TiO_2 process. After 30 min of reaction time, the initial antibiotic activity was reduced by 40%, and after 90 min of treatment, the inhibition zone was reduced by 100% [68]. In addition, Bouyarmane et al. [69] surveyed the degradation of OFL and CIP using TiO_2/hydroxyapatite nanocomposite under UV light. The authors reported that antibiotic-induced bacterial inhibition for CIP and OFL experienced a reducing trend and were 34 and 26 mm, respectively. Moreover, no *Escherichia coli* were detected in the effluents [69]. In another study, Mohan and Balakrishnan [70] reported that antibiotic-induced bacterial inhibition for *Escherichia coli* experience a decreasing trend in aquatic solution containing CIP after treatment with ozonation (reaction time = 25 min); antibiotic-induced bacterial inhibition was 23 mm at the start of reaction and this decreased to 6 mm.

3.9. Biological post-treatment

According to Fig. S2, the mineralization reached 37.5% after 30 min and the BOD_5/COD ratio was at 0.45. Contrarily, UV/iodide effluent includes a sizable number of metabolites with significant concentrations of biodegradable components. Because experts have said that biodegradation is a suggested strategy for mineralizing biodegradable organic compounds, a bioreactor may also assist in the mineralization of all intermediate products [24,51]. Shoorangiz et al. [71] reported that BOD_5/COD index of solution containing ciprofloxacin increased to 0.42 after 20 min reaction time with electro-Fenton process. Genç et al. [72] reported that photocatalytic oxidation improved the BOD_5/COD index of aquatic solution containing ciprofloxacin from 0.043 to 0.403 after 30 min of reaction time. Four factors were taken into consideration when choosing the effluent from CIP degradation by the UV/iodide method: (1) intermediate generated, (2) destruction rate, (3) bacterial susceptibility test, and (4) BOD_5/COD ratio. Because of the total decomposition of organic matter brought on by CIP degradation, biological treatment was applied to further decrease COD. The biological reactor received the photoreduction effluent, which reduced the COD from 96 to 60 mg·L^{-1}. A variety of MLSS were utilized in biological reactors. When bioreactor operated with MLSS 1000 the COD removal efficiency reached 63.8% (130 to 47 mg·L^{-1}) within 11 h, as shown in Fig. 10. However, when the concentration of MLSS increased to 3,000 mg·L^{-1} (from 185 to 39.7 mg·L^{-1}), the COD removal efficiency increased to 78.4%, and at 5,000 mg·L^{-1}, it increased to 88.16% (from 245 to 29 mg·L^{-1}). Although relatively economical, biological reactors cannot break down organic material that is resistant to or not biodegradable. On the other hand, full mineralization of organic molecules in photocatalytic reactors is not economically feasible due to their high energy consumption. Since all metabolites have been

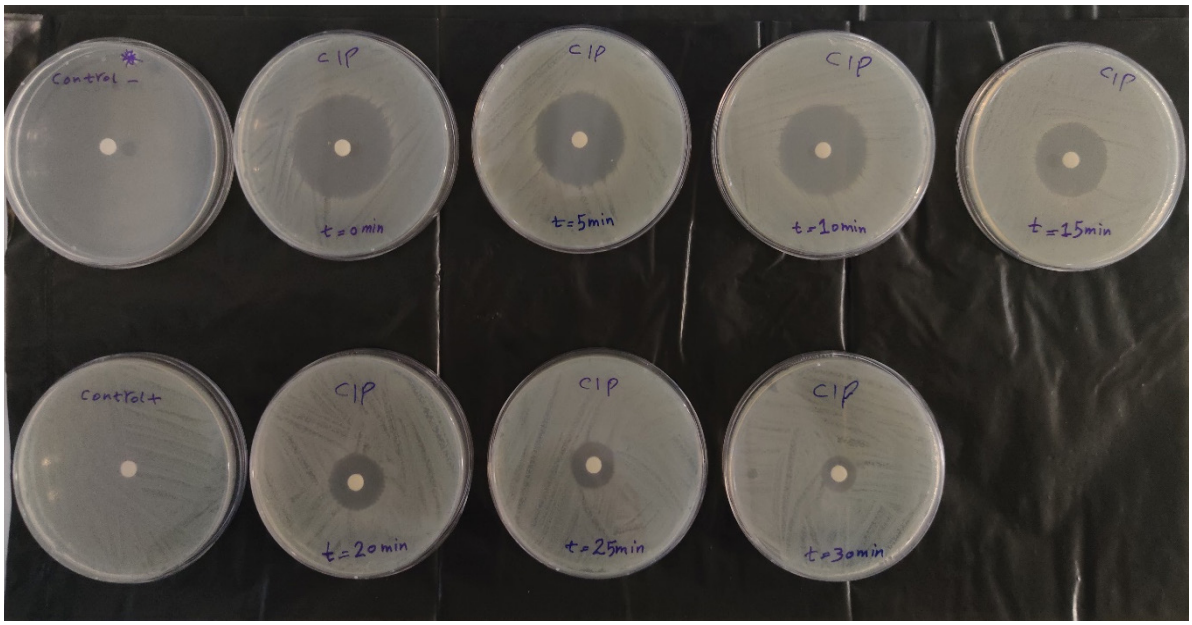

Fig. 9. Result of bacterial susceptibility test and antibiotic activity.

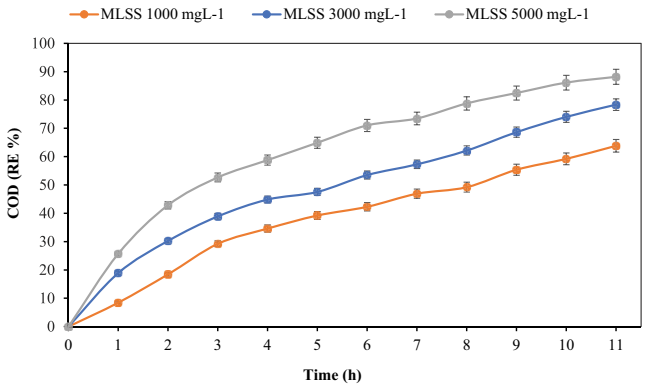

Fig. 10. Evaluation of chemical oxygen demand in biological post-treatment.

mineralized, continued usage of photocatalytic reactors and bioreactors has been shown to be both efficient and cost-effective. In other words, by quickly decomposing the intermediates created by the photocatalytic process, microbes enable the final effluent to be released into the environment by mineralizing their channels [73]. Sheikhmohammadi et al. [74] observed trichlorophenol COD reduction efficiencies up to 68.66%, 79.22%, and 86.9% in a 12-h biological reaction with 1,000; 3,000 and 5,000, respectively. Sarkhosh et al. [73] investigated the biological degradation of bisphenol removal, in order to further mineralize the final compounds produced in the photodegradation process. The results obtained from the biological process with at a fixed MLSS concentration equal to 3,500 mg·L^{-1} and different COD concentrations of 100, 200 and 300 mg·L^{-1} led to complete degradation of COD after 5, 9 and 14 h.

4. Conclusions

Numerous health issues caused by organic solvent resistant matter to biodegradation have forced communities to utilize cutting-edge techniques to address them. Additionally, the utilization of nanoparticle-based technologies (such as adsorption or advanced oxidation) would result in the production of a secondary pollutant, therefore worries regarding their existence cannot be disregarded. The purpose of this study is to investigate the effectiveness of the advanced UV/iodide regeneration process in improving the biological degradability of wastewater containing the antibiotic ofloxacin and the mineralization of most of the compounds produced in the photodegradation process in a biological reactor in order to reach the effluent standards. The kinetics of the reaction was investigated by the pseudo-first-order model method, and the reaction constant and reaction rate decreased with increasing concentration. The energy consumption was calculated by kinetic and IUPAC methods, which shows that in both models, the amount of energy consumption increased with increasing concentration. The effect of the main water anions on the performance of the UV/iodide process was investigated and the most negative effect on the process was found for nitrate, bicarbonate, sulfate and chloride. Reactive species were investigated using scavengers, and reducing species (hydrated electrons, hydrogen radicals) played an key roles in the photodegradation of pollutants. By examining the intermediate compounds identified, it was found that the cyclic compounds have been transformed into linear and simple organic and rapidly biodegradable compounds. Kirby–Bauer method was used to identify bacterial susceptibility of the UV/iodide process effluent and the results show a great decrease in the bacterial susceptibility of the treated effluent. The ratio of (BOD_5)/(COD) was obtained to 0.45 after the reaction time of 30 min, indicating the appropriate biodegradability of the effluent. The effluent of UV/iodide advanced reduction process entered to the biological reactor and 88%.16 was mineralized after 11 h of biological reaction time. As a consequence of this work, it is now possible to treat wastewater containing refractory organic materials, such as CIP, in an effective and ecologically beneficial manner by using a biological process that comes after the ARP procedure.

Acknowledgements

The present research was adapted from the Ph.D. Thesis of Norouz Mahmoudi at Iran University of Medical Sciences. The authors gratefully acknowledge the financial support given by Research Center for Environmental Health Technology, Iran University of Medical Sciences, Tehran, Iran (Grant Number 0-1-2-19983). (Ethics Code: IR.IUMS.REC.1400.057).

Conflicts of interest

The authors of this article declare that they have no conflict of interests.

References

[1] N. Cheng, B. Wang, P. Wu, X. Lee, Y. Xing, M. Chen, B. Gao, Adsorption of emerging contaminants from water and wastewater by modified biochar: a review, Environ. Pollut., 273 (2021) 116448, doi: 10.1016/j.envpol.2021.116448.
[2] N.A. Khan, V. Vambol, S. Vambol, B. Bolibrukh, M. Sillanpaa, F. Changani, A. Esrafili, M. Yousefi, Hospital effluent guidelines and legislation scenario around the globe: a critical review, J. Environ. Chem. Eng., 9 (2021) 105874, doi: 10.1016/j.jece.2021.105874.
[3] F. Wahid, S. Baig, M.F. Bhatti, M. Manzoor, I. Ahmed, M. Arshad, Growth responses and rubisco activity influenced by antibiotics and organic amendments used for stress alleviation in *Lactuca sativa*, Chemosphere, 264 (2021) 128433, doi: 10.1016/j.chemosphere.2020.128433.
[4] R. Mirzaei, M. Yunesian, S. Nasseri, M. Gholami, E. Jalilzadeh, S. Shoeibi, A. Mesdaghinia, Occurrence and fate of most prescribed antibiotics in different water environments of Tehran, Iran, Sci. Total. Environ., 619–620 (2018) 446–459.
[5] Y. Ben, C. Fu, M. Hu, L. Liu, M.H. Wong, C. Zheng, Human health risk assessment of antibiotic resistance associated with antibiotic residues in the environment: a review, Environ. Res., 169 (2019) 483–493.
[6] K. Yu, X. Li, L. Chen, J. Fang, H. Chen, Q. Li, N. Chi, J. Ma, Mechanism and efficiency of contaminant reduction by hydrated electron in the sulfite/iodide/UV process, Water Res., 129 (2018) 357–364.
[7] G. Feng, H. Huang, Y. Chen, Effects of emerging pollutants on the occurrence and transfer of antibiotic resistance genes: a review, J. Hazard. Mater., 420 (2021) 126602, doi: 10.1016/j.jhazmat.2021.126602.
[8] N.A. Khan, S.U. Khan, S. Ahmed, I.H. Farooqi, M. Yousefi, A.A. Mohammadi, F. Changani, Recent trends in disposal and treatment technologies of emerging-pollutants-a critical

review, TrAC, Trends Anal. Chem., 122 (2020) 115744, doi: 10.1016/j.trac.2019.115744.
[9] H.A. Ahmad, S. Ahmad, Q. Cui, Z. Wang, H. Wei, X. Chen, S.-Q. Ni, S. Ismail, H.M. Awad, A. Tawfik, The environmental distribution and removal of emerging pollutants, highlighting the importance of using microbes as a potential degrader: a review, Sci. Total Environ., 809 (2022) 151926, doi: 10.1016/j.scitotenv.2021.151926.
[10] X. Ao, W. Liu, W. Sun, M. Cai, Z. Ye, C. Yang, Z. Lu, C. Li, Medium pressure UV-activated peroxymonosulfate for ciprofloxacin degradation: kinetics, mechanism, and genotoxicity, Chem. Eng. J., 345 (2018) 87–97.
[11] M. Yousefi, M. Gholami, V. Oskoei, A.A. Mohammadi, M. Baziar, A. Esrafili, Comparison of LSSVM and RSM in simulating the removal of ciprofloxacin from aqueous solutions using magnetization of functionalized multi-walled carbon nanotubes: process optimization using GA and RSM techniques, J. Environ. Chem. Eng., 9 (2021) 105677, doi: 10.1016/j.jece.2021.105677.
[12] A. Dehghan, A.A. Mohammadi, M. Yousefi, A.A. Najafpoor, M. Shams, S. Rezania, Enhanced kinetic removal of ciprofloxacin onto metal-organic frameworks by sonication, process optimization and metal leaching study, Nanomaterials, 9 (2019) 1422, doi: 10.3390/nano9101422.
[13] H. Park, C.D. Vecitis, J. Cheng, N.F. Dalleska, B.T. Mader, M.R. Hoffmann, Reductive degradation of perfluoroalkyl compounds with aquated electrons generated from iodide photolysis at 254 nm, Photochem. Photobiol. Sci., 10 (2011) 1945–1953.
[14] N.H. Tran, H. Chen, M. Reinhard, F. Mao, K.Y.-H. Gin, Occurrence and removal of multiple classes of antibiotics and antimicrobial agents in biological wastewater treatment processes, Water Res., 104 (2016) 461–472.
[15] A.S. Ajibola, O.A. Amoniyan, F.O. Ekoja, F.O. Ajibola, QuEChERS approach for the analysis of three fluoroquinolone antibiotics in wastewater: concentration profiles and ecological risk in two Nigerian hospital wastewater treatment plants, Arch. Environ. Contam. Toxicol., 80 (2021) 389–401.
[16] R. Wajahat, A. Yasar, A.M. Khan, A.B. Tabinda, S.G. Bhatti, Ozonation and photo-driven oxidation of ciprofloxacin in pharmaceutical wastewater: degradation kinetics and energy requirements, Pol. J. Environ. Stud., 28 (2019) 1–6.
[17] P.Y. Motlagh, S. Akay, B. Kayan, A. Khataee, Ultrasonic assisted photocatalytic process for degradation of ciprofloxacin using TiO_2-Pd nanocomposite immobilized on pumice stone, J. Ind. Eng. Chem., 104 (2021) 582–591.
[18] Z. Chen, W. Lai, Y. Xu, G. Xie, W. Hou, P. Zhanchang, C. Kuang, Y. Li, Anodic oxidation of ciprofloxacin using different graphite felt anodes: kinetics and degradation pathways, J. Hazard. Mater., 405 (2021) 124262, doi: 10.1016/j.jhazmat.2020.124262.
[19] F. Du, Z. Lai, H. Tang, H. Wang, C. Zhao, Construction and application of BiOCl/Cu-doped Bi_2S_3 composites for highly efficient photocatalytic degradation of ciprofloxacin, Chemosphere, 287 (2022) 132391, doi: 10.1016/j.chemosphere.2021.132391.
[20] C.A. Igwegbe, S.N. Oba, C.O. Aniagor, A.G. Adeniyi, J.O. Ighalo, Adsorption of ciprofloxacin from water: a comprehensive review, J. Ind. Eng. Chem., 93 (2021) 57–77.
[21] A. Alinejad, H. Akbari, M. Ghaderpoori, A.K. Jeihooni, A. Adibzadeh, Catalytic ozonation process using a MgO nanocatalyst to degrade methotrexate from aqueous solutions and cytotoxicity studies in human lung epithelial cells (A549) after treatment, RSC Adv., 9 (2019) 8204–8214.
[22] B. Kamarehie, A. Jafari, M. Ghaderpoori, M. Amin Karami, K. Mousavi, A. Ghaderpoury, Catalytic ozonation process using PAC/γ-Fe_2O_3 to Alizarin Red S degradation from aqueous solutions: a batch study, Chem. Eng. Commun., 206 (2019) 898–908.
[23] M. Massoudinejad, H. Keramati, M. Ghaderpoori, Investigation of photo-catalytic removal of arsenic from aqueous solutions using UV/H_2O_2 in the presence of ZnO nanoparticles, Chem. Eng. Commun., 207 (2020) 1605–1615.
[24] H. Azarpira, M. Sadani, M. Abtahi, N. Vaezi, S. Rezaei, Z. Atafar, S.M. Mohseni, M. Sarkhosh, M. Ghaderpoori, H. Keramati, R. Hosseini Pouya, A. Akbari, V. Fanai, Photo-catalytic degradation of triclosan with UV/iodide/ZnO process: performance, kinetic, degradation pathway, energy consumption and toxicology, J. Photochem. Photobiol., A, 371 (2019) 423–432.
[25] B. Kamarehie, M. Ghaderpoori, A. Ghaderpoury, A. Alinejadg, R. Heydari, Catalytic ozonation process using MgO-PAC to degrade Bisphenol A from aqueous solutions, Desal. Water Treat., 184 (2020) 232–242.
[26] M. Dolatabadi, T. Świergosz, C. Wang, S. Ahmadzadeh, Accelerated degradation of groundwater-containing malathion using persulfate activated magnetic Fe_3O_4/graphene oxide nanocomposite for advanced water treatment, Arabian J. Chem., 16 (2023) 104424, doi: 10.1016/j.arabjc.2022.104424.
[27] Z. Sun, C. Zhang, P. Chen, Q. Zhou, M.R. Hoffmann, Impact of humic acid on the photoreductive degradation of perfluorooctane sulfonate (PFOS) by UV/iodide process, Water Res., 127 (2017) 50–58.
[28] J. Zhang, H. Zhang, X. Liu, F. Cui, Z. Zhao, Efficient reductive and oxidative decomposition of haloacetic acids by the vacuum-ultraviolet/sulfite system, Water Res., 210 (2022) 117974, doi: 10.1016/j.watres.2021.117974.
[29] T. Rasolevandi, S. Naseri, H. Azarpira, A. Mahvi, Photodegradation of dexamethasone phosphate using UV/iodide process: kinetics, intermediates, and transformation pathways, J. Mol. Liq., 295 (2019) 111703, doi: 10.1016/j.molliq.2019.111703.
[30] M. Massoudinejad, S.M. Zarandi, M.M. Amini, S.M. Mohseni, Enhancing photo-precipitation of chromate with carboxyl radicals: kinetic, energy analysis and sludge survey, Process Saf. Environ. Prot., 134 (2020) 440–447.
[31] L. Lehr, M. Zanni, C. Frischkorn, R. Weinkauf, D. Neumark, Electron solvation in finite systems: femtosecond dynamics of iodide. (Water)n anion clusters, Science, 284 (1999) 635–638.
[32] H.A. Schwarz, Free radicals generated by radiolysis of aqueous solutions, J. Chem. Educ., 58 (1981) 101, doi: 10.1021/ed058p101.
[33] H. Tian, Y. Guo, B. Pan, C. Gu, H. Li, S.A. Boyd, Enhanced photoreduction of nitro-aromatic compounds by hydrated electrons derived from indole on natural montmorillonite, Environ. Sci. Technol., 49 (2015) 7784–7792.
[34] S. Azizi, M. Sarkhosh, A.A. Najafpoor, S.M. Mohseni, M. Mazza, M. Sadani, Degradation of Codeine Phosphate by simultaneous usage of e^-_{aq} and •OH radicals in photo-redox processes: influencing factors, energy consumption, kinetics, intermediate products and degradation pathways, Optik, 243 (2021) 167415, doi: 10.1016/j.ijleo.2021.167415.
[35] H. Azarpira, M. Abtahi, M. Sadani, S. Rezaei, Z. Atafar, S.M. Mohseni, M. Sarkhosh, M. Shanbedi, H. Alidadi, Y. Fakhri, Photo-catalytic degradation of trichlorophenol with UV/sulfite/ZnO process, simultaneous usage of homogeneous reductive and heterogeneous oxidative agents generator as a new approach of advanced oxidation/reduction processes (AO/RPs), J. Photochem. Photobiol., A, 374 (2019) 43–51.
[36] P. Calza, E. Pelizzetti, Reactivity of chloromethanes with photogenerated hydrated electrons, J. Photochem. Photobiol., A, 162 (2004) 609–613.
[37] J.A. Khan, N.S. Shah, S. Nawaz, M. Ismail, F. Rehman, H.M. Khan, Role of e^-_{aq}, •OH and H• in radiolytic degradation of atrazine: A kinetic and mechanistic approach, J. Hazard. Mater., 288 (2015) 147–157.
[38] M. Sarkhosh, M. Sadani, M. Abtahi, S.M. Mohseni, A. Sheikhmohammadi, H. Azarpira, A.A. Najafpoor, Z. Atafar, S. Rezaei, R. Alli, A. Bay, Enhancing photodegradation of ciprofloxacin using simultaneous usage of e^-_{aq} and •OH over UV/ZnO/I^- process: efficiency, kinetics, pathways, and mechanisms, J. Hazard. Mater., 377 (2019) 418–426.
[39] H. Nishiyama, H. Ikeda, T. Saito, B. Kriegel, H. Tsurugi, J. Arnold, K. Mashima, Structural and electronic noninnocence of α-diimine ligands on niobium for reductive C–Cl bond activation and catalytic radical addition reactions, J. Am. Chem. Soc., 139 (2017) 6494–6505.
[40] K. López-Velázquez, J.L. Guzmán-Mar, H.A. Saldarriaga-Noreña, M.A. Murillo-Tovar, L. Hinojosa-Reyes, M. Villanueva-Rodríguez, Occurrence and seasonal distribution of five selected endocrine-disrupting compounds in wastewater treatment plants of the Metropolitan Area of Monterrey, Mexico: the role of water quality parameters, Environ. Pollut., 269 (2021) 116223, doi: 10.1016/j.envpol.2020.116223.

[41] G. Moussavi, M. Pourakbar, S. Shekoohiyan, M. Satari, The photochemical decomposition and detoxification of Bisphenol A in the VUV/H_2O_2 process: degradation, mineralization, and cytotoxicity assessment, Chem. Eng. J., 331 (2018) 755–764.
[42] C.-G. Lee, H. Javed, D. Zhang, J.-H. Kim, P. Westerhoff, Q. Li, P.J. Alvarez, Porous electrospun fibers embedding TiO_2 for adsorption and photocatalytic degradation of water pollutants, Environ. Sci. Technol., 52 (2018) 4285–4293.
[43] Y. Qi, J. Wei, R. Qu, G. Al-Basher, X. Pan, A.A. Dar, A. Shad, D. Zhou, Z. Wang, Mixed oxidation of aqueous nonylphenol and triclosan by thermally activated persulfate: reaction kinetics and formation of co-oligomerization products, Chem. Eng. J., 403 (2021) 126396, doi: 10.1016/j.cej.2020.126396.
[44] M. He, Z. Wan, D.C.W. Tsang, Y. Sun, E. Khan, D. Hou, N.J.D. Graham, Performance indicators for a holistic evaluation of catalyst-based degradation—a case study of selected pharmaceuticals and personal care products (PPCPs), J. Hazard. Mater., 402 (2021) 123460, doi: 10.1016/j.jhazmat.2020.123460.
[45] R.K. Singh, L. Philip, S. Ramanujam, Rapid degradation, mineralization and detoxification of pharmaceutically active compounds in aqueous solution during pulsed corona discharge treatment, Water Res., 121 (2017) 20–36.
[46] A.P.H. Association, A.W.W. Association, Standard Methods for the Examination of Water and Wastewater, 1995, pp. 1000–1000.
[47] A. Samzadeh, M. Dehghani, M.A. Baghapour, A. Azhdarpoor, Z. Derakhshan, M. Cvetnić, T. Bolanča, S. Giannakis, Y. Cao, Comparative photo-oxidative degradation of etodolac, febuxostat and imatinib mesylate by UV-C/H_2O_2 and UV-C/$S_2O_8^{2-}$ processes: modeling, treatment optimization and biodegradability enhancement, Environ. Res., 212 (2022) 113385, doi: 10.1016/j.envres.2022.113385.
[48] Z. Sun, C. Zhang, X. Zhao, J. Chen, Q. Zhou, Efficient photoreductive decomposition of N-nitrosodimethylamine by UV/iodide process, J. Hazard. Mater., 329 (2017) 185–192.
[49] V.S.V. Botlaguduru, B. Batchelor, A. Abdel-Wahab, Application of UV–sulfite advanced reduction process to bromate removal, J. Water Process Eng., 5 (2015) 76–82.
[50] H. Milh, X. Yu, D. Cabooter, R. Dewil, Degradation of ciprofloxacin using UV-based advanced removal processes: comparison of persulfate-based advanced oxidation and sulfite-based advanced reduction processes, Sci. Total Environ., 764 (2021) 144510, doi: 10.1016/j.scitotenv.2020.144510.
[51] M. Sarkhosh, M. Sadani, M. Abtahi, S.M. Mohseni, A. Sheikhmohammadi, H. Azarpira, A.A. Najafpoor, Z. Atafar, S. Rezaei, R. Alli, Enhancing photodegradation of ciprofloxacin using simultaneous usage of e^-_{aq} and •OH over UV/ZnO/I^- process: efficiency, kinetics, pathways, and mechanisms, J. Hazard. Mater., 377 (2019) 418–426.
[52] X. Li, J. Fang, G. Liu, S. Zhang, B. Pan, J. Ma, Kinetics and efficiency of the hydrated electron-induced dehalogenation by the sulfite/UV process, Water Res., 62 (2014) 220–228.
[53] B. Xie, X. Li, X. Huang, Z. Xu, W. Zhang, B. Pan, Enhanced debromination of 4-bromophenol by the UV/sulfite process: efficiency and mechanism, J. Environ. Sci., 54 (2017) 231–238.
[54] B. Jung, R. Nicola, B. Batchelor, A. Abdel-Wahab, Effect of low- and medium-pressure Hg UV irradiation on bromate removal in advanced reduction process, Chemosphere, 117 (2014) 663–672.
[55] X. Yu, D. Cabooter, R. Dewil, Effects of process variables and kinetics on the degradation of 2,4-dichlorophenol using advanced reduction processes (ARP), J. Hazard. Mater., 357 (2018) 81–88.
[56] M. Dolatabadi, M.H. Ehrampoush, M. Pournamdari, A.A. Ebrahimi, H. Fallahzadeh, S. Ahmadzadeh, Simultaneous electrochemical degradation of pesticides from the aqueous environment using Ti/SnO_2–Sb_2O_3/PbO_2/Bi electrode; process modeling and mechanism insight, Chemosphere, 311 (2023) 137001, doi: 10.1016/j.chemosphere.2022.137001.
[57] A. Rahmah, S. Harimurti, T. Murugesan, Experimental investigation on the effect of wastewater matrix on oxytetracycline mineralization using UV/H_2O_2 system, Int. J. Environ. Sci. Technol., 14 (2017) 1225–1233.
[58] A. Bianco Prevot, C. Baiocchi, M.C. Brussino, E. Pramauro, P. Savarino, V. Augugliaro, G. Marcì, L. Palmisano, Photocatalytic degradation of Acid Blue 80 in aqueous solutions containing TiO_2 suspensions, Environ. Sci. Technol., 35 (2001) 971–976.
[59] E.M. Elsaid, I. Ibrahim, T.Z.A. Wahid, Kinetic and thermodynamic examinations for the unsteady couette flow problem of a plasma using the BGK cylindrical model, Chin. J. Phys., 77 (2022) 161–175.
[60] H. Wang, L. Wang, D. Lin, X. Feng, Y. Niu, B. Zhang, F.-S. Xiao, Strong metal–support interactions on gold nanoparticle catalysts achieved through Le Chatelier's principle, Nat. Catal., 4 (2021) 418–424.
[61] G. Moussavi, M. Rezaei, M. Pourakbar, Comparing VUV and VUV/Fe^{2+} processes for decomposition of cloxacillin antibiotic: degradation rate and pathways, mineralization and by-product analysis, Chem. Eng. J., 332 (2018) 140–149.
[62] L. Wang, D. Kong, Y. Ji, J. Lu, X. Yin, Q. Zhou, Transformation of iodide and formation of iodinated by-products in heat activated persulfate oxidation process, Chemosphere, 181 (2017) 400–408.
[63] C. Liu, V. Nanaboina, G.V. Korshin, W. Jiang, Spectroscopic study of degradation products of ciprofloxacin, norfloxacin and lomefloxacin formed in ozonated wastewater, Water Res., 46 (2012) 5235–5246.
[64] Y. Wang, D. Tian, W. Chu, M. Li, X. Lu, Nanoscaled magnetic $CuFe_2O_4$ as an activator of peroxymonosulfate for the degradation of antibiotics norfloxacin, Sep. Purif. Technol., 212 (2019) 536–544.
[65] D. Kamath, S.P. Mezyk, D. Minakata, Elucidating the elementary reaction pathways and kinetics of hydroxyl radical-induced acetone degradation in aqueous phase advanced oxidation processes, Environ. Sci. Technol., 52 (2018) 7763–7774.
[66] M. Feng, X. Wang, J. Chen, R. Qu, Y. Sui, L. Cizmas, Z. Wang, V.K. Sharma, Degradation of fluoroquinolone antibiotics by ferrate(VI): effects of water constituents and oxidized products, Water Res., 103 (2016) 48–57.
[67] Z. Wang, X. Cai, X. Xie, S. Li, X. Zhang, Z. Wang, Visible-LED-light-driven photocatalytic degradation of ofloxacin and ciprofloxacin by magnetic biochar modified flower-like Bi_2WO_6: the synergistic effects, mechanism insights and degradation pathways, Sci. Total Environ., 764 (2021) 142879, doi: 10.1016/j.scitotenv.2020.142879.
[68] A. Chatzitakis, C. Berberidou, I. Paspaltsis, G. Kyriakou, T. Sklaviadis, I. Poulios, Photocatalytic degradation and drug activity reduction of chloramphenicol, Water Res., 42 (2008) 386–394.
[69] H. Bouyarmane, C. El Bekkali, J. Labrag, I. Es-saidi, O. Bouhnik, H. Abdelmoumen, A. Laghzizil, J.M. Nunzi, D. Robert, Photocatalytic degradation of emerging antibiotic pollutants in waters by TiO_2/hydroxyapatite nanocomposite materials, Surf. Interfaces, 24 (2021) 101155, doi: 10.1016/j.surfin.2021.101155.
[70] S. Mohan, P. Balakrishnan, Kinetics of ciprofloxacin removal using a sequential two-step ozonation-biotreatment process, Environ. Technol. Innovation, 21 (2021) 101284, doi: 10.1016/j.eti.2020.101284.
[71] M. Shoorangiz, M.R. Nikoo, M. Salari, G.R. Rakhshandehroo, M. Sadegh, Optimized electro-Fenton process with sacrificial stainless steel anode for degradation/mineralization of ciprofloxacin, Process Saf. Environ. Prot., 132 (2019) 340–350.
[72] N. Genç, Improvement of the overall biodegradability of ciprofloxacin by pre-treatment with photocatalytic oxidation of wastewaters, Asian J. Water Environ. Pollut., 13 (2016) 75–81.
[73] M. Sarkhosh, M. Sadani, M. Abtahi, H. Azarpira, H. Alidadi, Z. Atafar, S. Rezaei, S.M. Mohseni, N. Vaezi, Y. Fakhri, H. Keramati, Photo-biological degradation of Bisphenol A, UV/ZnO/iodide process at the center of biological reactor, J. Photochem. Photobiol., A, 374 (2019) 115–124.
[74] A. Sheikhmohammadi, A. Yazdanbakhsh, G. Moussavi, A. Eslami, M. Rafiee, M. Sardar, M. Almasian, Degradation and COD removal of trichlorophenol from wastewater using sulfite anion radicals in a photochemical process combined with a biological reactor: mechanisms, degradation pathway, optimization and energy consumption, Process Saf. Environ. Prot., 123 (2019) 263–271.

Supporting information

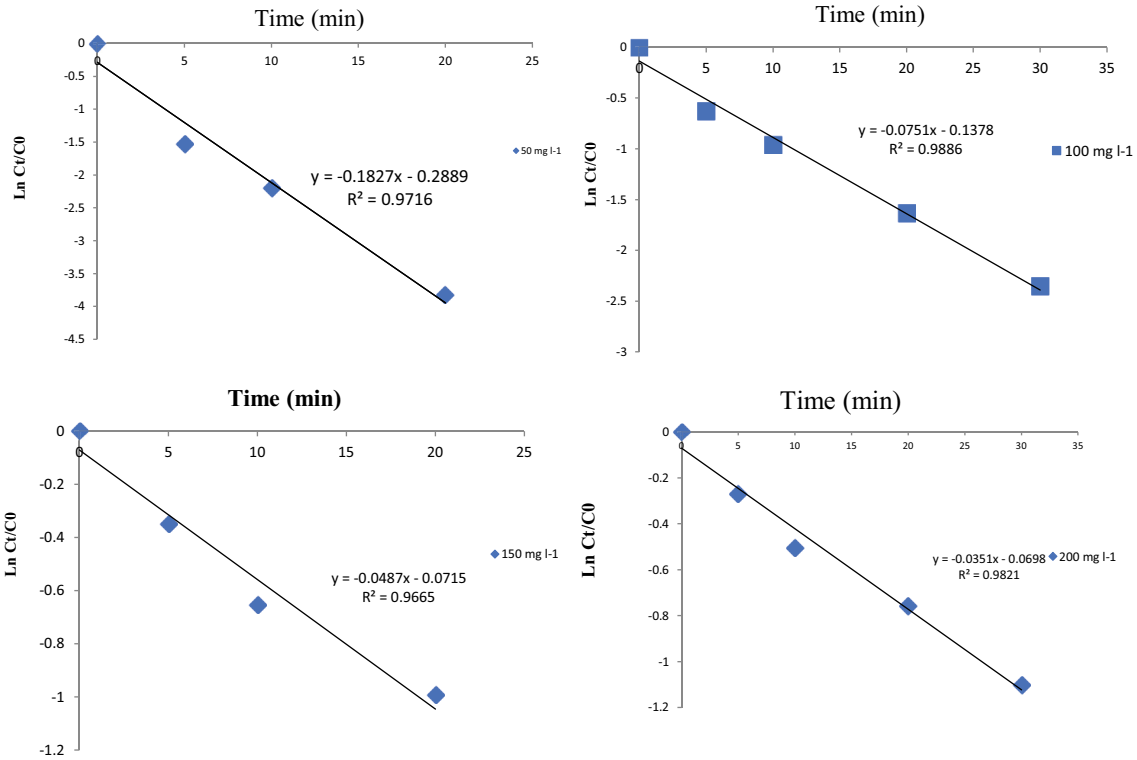

Fig. S1. Drawing $\ln C_t/C_0$ ciprofloxacin vs. time to obtain reaction constant (k_{obs}) at a concentration of 50–200 mg·L^{-1}.

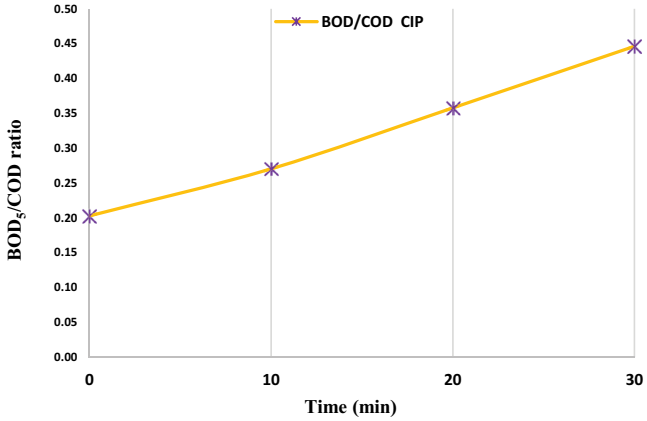

Fig. S2. BOD_5/COD ratio of effluent from ciprofloxacin treatment by UV/iodide process.